 doi:10.20944/preprints202204.0248.v1

Joint Transcriptome and Metabolome Analysis Prevails Biological Mechanisms Underlying the Prosurvival Fight in Heat Stressed Granulosa Cells

Abdul Sammad[1], Hanpeng Luo[1], Lirong Hu[1], Adnan Khan[1], Huabin Zhu [2,*] and Yachun Wang [1,*]

[1] National Engineering Laboratory for Animal Breeding, Key Laboratory of Animal Genetics, Breeding and Reproduction, MARA, College of Animal Sciences and Technology, China Agricultural University, 100193, Beijing, China
[2] Embryo Biotechnology and Reproduction Laboratory, Institute of Animal Sciences, Chinese Academy of Agricultural Sciences, 100193, Beijing, China
* Correspondence: Y.W, wangyachun@cau.edu.cn, H.Z, zhuhuabin@caas.cn

Abstract: Previous studies reported the physical, transcriptomics and metabolomics changes in in-vitro acute heat stressed bovine granulosa cells. Granulosa cells exhibited transient proliferation senescence, oxidative stress, increased rate of apoptosis, and decline in steroidogenic activity. This study performs joint integration and network analysis of metabolomics and transcriptomics data to further narrow down and elucidate the role of differentially expressed genes, important metabolites and relevant cellular and metabolic pathways in acute heat-stressed granulosa cells. Among significant (Raw *P*-value <0.05) metabolic pathways where metabolites and genes did converge, this study found Vitamin B6 metabolism, Glycine, serine and threonine metabolism, Phenylalanine metabolism, Arginine biosynthesis, Tryptophan metabolism, Arginine and proline metabolism, Histidine metabolism, and Glyoxylate and dicarboxylate metabolism. Important significant convergent biological pathways included, ABC transporters and Protein digestion and absorption, while functional signaling pathways included cAMP, mTOR, and AMPK signaling pathways together with Ovarian steroidogenesis pathway. Among caner pathways, the most important pathway was Central carbon metabolism in cancer. Through multiple analysis query, Progesterone, Serotonin, citric acid, Pyridoxal, L-Lysine, Succinic acid, L-Glutamine, L-Leucine, L-Threonine, L-Tyrosine, Vitamin B6, Choline, and *CYP1B1*, *MAOB*, *VEGFA*, *WNT11*, *AOX1*, *ADCY2*, *ICAM1*, *PYGM*, *SLC2A4*, *SLC16A3*, *HSD11B2* and *NOS2* appeared to be important enriched metabolites and genes, respectively. These genes, metabolites, metabolic, cellular and cell signaling pathways comprehensively elucidate the mechanisms underlying the intricate fight between death and survival in acute heat-stressed bovine granulosa cells, and essentially help further our understanding and future quest of research in this direction.

Keywords: granulosa cells; heat stress; integrated analysis; transcriptomics; metabolomics; differentially expressed genes; metabolites; signaling pathways; metabolic pathways; cancer pathways

1. Introduction

Ovarian granulosa cells present in the follicles nurtures oocyte and have a specialized steroidogenesis role of steroidogenesis in ovaries [1,2]. Heat stress has been shown to alter granulosa cells survival, limit cell proliferation transition, decrease steroid hormones synthesis and secretion, cause oxidative stress, and promote apoptotic manifestation [3–5]. Impairment of granulosa cells through heat or occupational hazard stress leads to disruption of ovarian activity and oocyte development competence [6–8]. Higher ambient temperatures are shown to associate with decrease in ovarian reserves and reproductive aging [9]. Heat stress is also shown to advance the process of leutinization-differentiation in granulosa cells, a condition associated with decline in fertility [10]. Heat stress causes several metabolic changes in the body [11], where high ketone bodies, high non-esterified fatty acids, and inflammatory changes disrupts the biochemical profile in ovarian follicles [12–16]. Heat stress caused changes in biochemical profile of ovarian follicles have been

Preprints (www.preprints.org) | NOT PEER-REVIEWED | Posted: 27 April 2022 doi:10.20944/preprints202204.0248.v1

associated with dysfunction of granulosa cells and poor development of oocyte [16–18]. Earlier studies about heat stress in granulosa cells, reported a proliferation senescence and variable potential of granulosa cells to resume proliferation, following acute heat stress exposures [19,20]. In our previous heat stress study in granulosa cells [4], a despaired response was observed, where 40 °C appeared somewhat lethal than 41 °C. Although not representative of actual physiological conditions, simulating an in vitro acute heat stressed (43 °C for 2 h) bovine granulosa cell model will be helpful to grasp the real-time biological insights into the cellular stress responses at molecular level. Therefore, we performed another comprehensive study of acute heat stress (43 °C) to granulosa cells where a transient cellular senescence and later resumption of proliferation was observed in heat stressed granulosa cells. Our previous transcriptome level studies involving extensive range of temperatures gave useful biological insights into the cellular mechanisms, metabolic level changes and apoptotic and antioxidant pathways [4,21]. While in our LC-MS based untargeted metabolomics study, important metabolites, metabolic pathways and their interplay in cellular mechanisms were reported in acute heat stressed bovine granulosa cells [22]. Our transcriptome study reported evidences of an intricate fight between pro-survival and pro-death pathways, while metabolome study suggested differential metabolites directed towards bioenergetics support mechanisms in acute heat stressed bovine granulosa cells [21,22]. Integrated transcriptome and metabolome analyses involving correlation and network analysis, is an efficient strategy to explore the mechanisms underlying a biological system. Therefore, this study intends to evaluate cellular physical responses and integrate the transcriptome and metabolome data from acute heat stressed bovine granulosa cells [21,22], to narrow down and possibly explore new biological insights regarding important genes, metabolites, adaptive pathways involved in aftermath of acute heat stress to bovine granulosa cells.

2. Results

2.1. Effect of heat stress on granulosa cell parameters

Bovine granulosa were exposed to in vitro heat stress treatment (43 °C), while the control group remained at 38 °C [21,22]. Cells in the control group maintained steady proliferation activity (Figure 1A), while no change was observed until 24 h in treatment group (Figure 1A). Significant ($p < 0.05$) difference in cell viability was observed at 24 and 48 h time points between both groups. A significant increase in ROS level was observed in the treatment group, compared to control group (Figure 1B). Similarly, heat stressed GCs had a significantly higher ($p < 0.05$) apoptotic rate (Figure 1F), as shown in representative fluorescent microphotographs of early apoptotic and late apoptotic events in the control group (Figure 1D) and heat stress (Figure 1E), respectively. Similarly, E2 and P4 levels were significantly ($p < 0.05$) decreased in the culture media of the treatment group (Figure 1C and 1G, respectively).

Preprints (www.preprints.org) | NOT PEER-REVIEWED | Posted: 27 April 2022 doi:10.20944/preprints202204.0248.v1

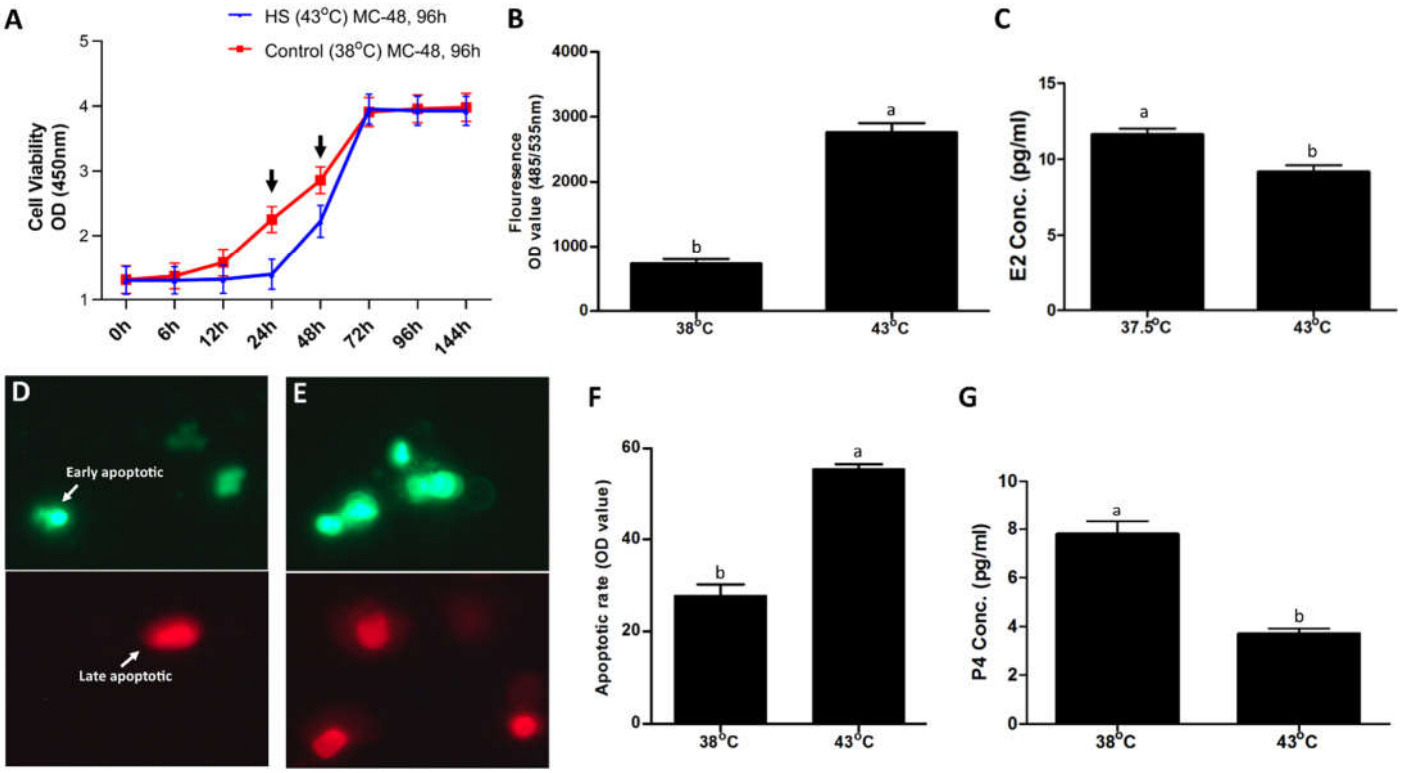

Figure 1. Comparison of physical parameters of bovine granulosa cells in heat stress (43 °C for 2 h) versus control (38 °C) [21,22]. Granulosa cells proliferation curves with mean optical densities (ODs) are plotted against different recovery time points in hours (h) for both groups, where cell viability at time point with arrows upon them are significantly ($p < 0.05$) different (1A). Fluorescence microscope pictures (200×) of late apoptotic (red) and early apoptotic (green) cells after stained with FITC/PI for control (1D) and treatment (1E) groups. Mean comparison of apoptotic rate (sum of red and green events) in cells among both groups (1F). Fluorocolorimetric OD values of reactive oxygen species (ROS) in cells are shown on the y-axis, and treatments are indicated on the x-axis (1B). Estrogen (E2) and Progesterone (P4) levels among control and treatment groups (1C, 1G), respectively. All data are represented as means ± S.E., means without common letters (a, b) are significantly different ($p < 0.05$).

2.2. Transcriptome and Metabolome from heat stressed granulosa cells

Total 256 significant differentially expressed genes (DEGs) and 51 differentially expressed important metabolites along with their logFC values were found in RNA sequencing analysis and LC-MS based untargeted metabolome analysis, respectively, which are used in this study for integrated analysis of transcriptome and metabolome underlying the biological mechanisms of acute heat stressed (43 °C for 2 h) bovine granulosa cells. This data came from our previous transcriptome and metabolome investigation performed on same samples replicates of the acute heat stressed granulosa cells. The principle component analysis (PCA) scores plot of transcriptome data, the partial least square-discriminate analysis (PLS-DA) scores plots for metabolites are given in supplementary figure S1. While, the list of significantly differentially expressed genes and metabolites along with their logFC values, used in this study are given in supplementary table S1.

2.3. Integrated pathways analysis of genes and metabolites

2.3.1. Joint pathways enrichment of genes used in this study

Differentially expressed genes of the transcriptomics data used in integrated analysis of this study were subjected to KEGG pathways based enrichment analysis, results of pathway analysis are illustrated in Figure 2.

Preprints (www.preprints.org) | NOT PEER-REVIEWED | Posted: 27 April 2022 doi:10.20944/preprints202204.0248.v1

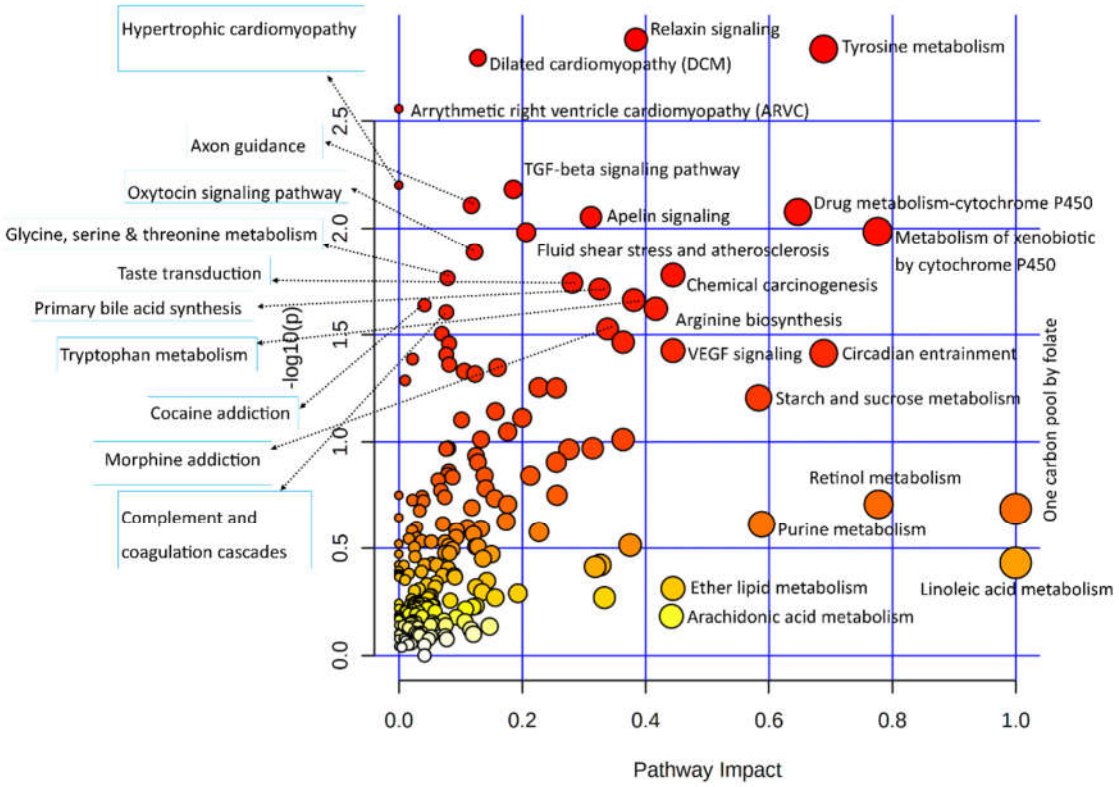

Figure 2. Dot plot illustration of pathways enrichment of significant differentially expressed genes used in this study. Various pathways with in upper and left quadrants are labelled. Size of dots increase with increasing pathway impact, while color intensifies according to y-axis.

Statistical results of transcriptomics enriched pathways analysis and list of enriched genes in each of these pathways are given in supplementary table S2. Out of functional pathways TGF-beta and VEGF signaling pathways were important, while numerous cellular processes pathways include Relaxin signaling, Cytochrome P450 pathways, Apelin signaling, Circadian entrainment, Chemical carcinogenesis, dilated cardiomyopathy, Axon guidance pathways enriched among bovine granulosa cells in response to acute heat stress. Large number of metabolic pathways were enriched in this integration analysis, out of which amino acid metabolic pathways were numerous including Tyrosine metabolism, Arginine biosynthesis, Glycine, serine, threonine metabolism, and Tryptophan metabolism were important. In carbohydrate metabolism pathways, Starch and sucrose metabolism pathway was enriched. Last important component of integration analysis includes lipids metabolism, where Linoleic acid metabolism, Ether lipid metabolism, and Arachidonic acid metabolism pathways were enriched. Similarly, all differential metabolites of metabolome data were also subjected to KEGG based pathway enrichment analysis, as shown in the illustration in Figure 3, while the statistical details of analysis and list of enriched metabolites are given in supplementary table S3. In only metabolites pathways analysis, aside of Aminoacyl-tRNA biosynthesis, major pathways enriched comprised of amino acids metabolism. Other important pathways were Vitamin B6 metabolism, Riboflavin metabolism and Citrate (TCA) cycle.

Preprints (www.preprints.org) | NOT PEER-REVIEWED | Posted: 27 April 2022 doi:10.20944/preprints202204.0248.v1

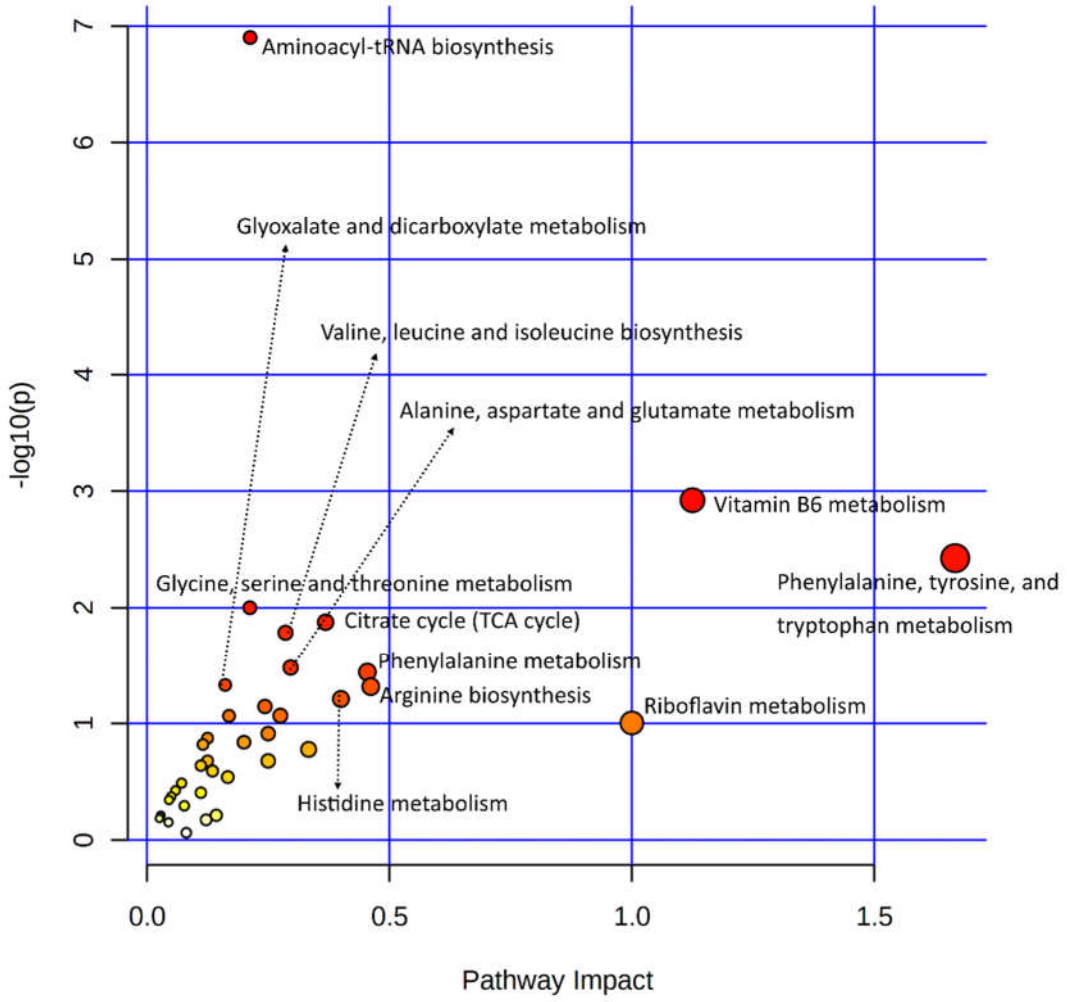

Figure 3. Dot plot illustration of pathways enrichment by significant differentially expressed metabolites used in this study. Various pathways within upper and left quadrants are labelled. Size of dots increase with increasing pathway impact, while color intensifies according to y-axis.

2.3.2. Combined pathway enrichment of genes and metabolites

Significant DEGs and important metabolites found in heat-stressed granulosa cells were subjected to integrated KEGG based pathways enrichment analysis as illustrated in Figure 4. As shown in Figure 4, ABC transporters, Central carbon metabolism, Aminoacyl-tRNA synthesis, Protein digestion and absorption, and Glycine, serine, threonine metabolism pathways were significantly enriched in response to heat stress treatment in bovine granulosa cells. Similarly, the pathways with most biological impact in molecular processes employed by granulosa cells to acute heat stress comprised of One carbon pool by folate, Vitamin B6 metabolism, Arginine and Tyrosine metabolism pathways.

Preprints (www.preprints.org) | NOT PEER-REVIEWED | Posted: 27 April 2022 doi:10.20944/preprints202204.0248.v1

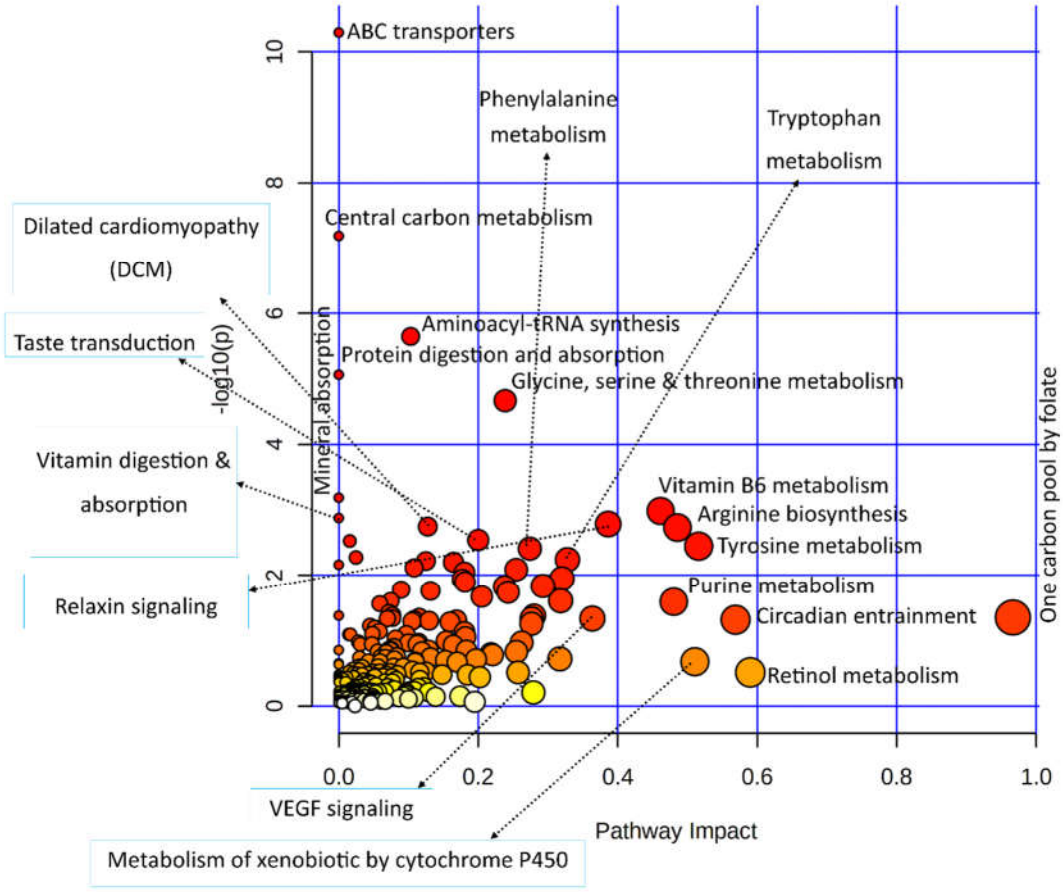

Figure 4. Dot plot illustration of pathways enrichment in integrated analysis of significant differentially expressed genes and important metabolites from transcriptome and metabolome data, respectively. Various pathways with in upper and left quadrants are labelled. Size of dots increase with increasing pathway impact, while color intensifies according to y-axis.

Statistical summary results of top enriched pathway of integrated analysis are detailed in Table 1, while the detailed results of all enriched pathways along with the list of enriched genes and metabolites in each of these pathways are listed in supplementary table S4.

Preprints (www.preprints.org) | NOT PEER-REVIEWED | Posted: 27 April 2022 doi:10.20944/preprints202204.0248.v1

Table 1. Statistical summary of top 25 metabolic and cellular pathways found in integrated joint pathways analysis of significant differentially expressed genes and important metabolites found in heat-stressed granulosa cells.

Pathways	Total /Hits	Raw *P*-value	Holm adjust *P*-value
ABC transporters	198/18	5.1E-11	1.7E-08
Central carbon metabolism in cancer	103/11	6.5E-08	2.1E-05
Aminoacyl-tRNA biosynthesis	118/10	2.3E-06	7.4E-04
Protein digestion and absorption	168/11	8.7E-06	2.8E-03
Glycine, serine and threonine metabolism	93/8	2.2E-05	7.0E-03
Mineral absorption	84/6	6.5E-04	2.1E-01
Vitamin B6 metabolism	36/4	1.0E-03	3.3E-01
Vitamin digestion and absorption	65/5	1.3E-03	4.3E-01
Relaxin signaling pathway	136/7	1.6E-03	5.3E-01
Dilated cardiomyopathy (DCM)	102/6	1.8E-03	5.7E-01
Arginine biosynthesis	42/4	1.9E-03	5.9E-01
Taste transduction	112/6	2.9E-03	9.1E-01
Arrhythmogenic right ventricular cardiomyopathy (ARVC)	78/5	3.0E-03	9.4E-01
Tyrosine metabolism	117/6	3.6E-03	1.00000
Phenylalanine metabolism	83/5	3.9E-03	1.00000
Cocaine addiction	56/4	5.3E-03	1.00000
Tryptophan metabolism	129/6	5.8E-03	1.00000
Glyoxylate and dicarboxylate metabolism	92/5	6.1E-03	1.00000
TGF-beta signaling pathway	93/5	6.3E-03	1.00000
Hypertrophic cardiomyopathy (HCM)	95/5	6.9E-03	1.00000
Axon guidance	180/7	7.7E-03	1.00000
GABAergic synapse	99/5	8.2E-03	1.00000
Alanine, aspartate and glutamate metabolism	65/4	9.0E-03	1.00000
Apelin signaling pathway	149/6	1.1E-02	1.00000
Histidine metabolism	70/4	1.2E-02	1.00000

2.3.3. Joint metabolic pathways analysis

Since number of important metabolites found in the metabolome of heat-stressed granulosa cells are less in number. Joint pathway analysis of both data involving only metabolic pathways, was also carried out (Figure 5). While, the statistical details and enriched genes or metabolites found in each of the enriched metabolic pathways are given in supplementary table S5. Results of this analysis did gave additional insights into the granulosa cells metabolic pathways employed in response to acute heat stress, where additional metabolic pathways observed included Arginine and proline metabolism, Drug metabolism by cytochrome P450, and Alanine, aspartate, glutamate metabolism were found.

Preprints (www.preprints.org) | NOT PEER-REVIEWED | Posted: 27 April 2022 doi:10.20944/preprints202204.0248.v1

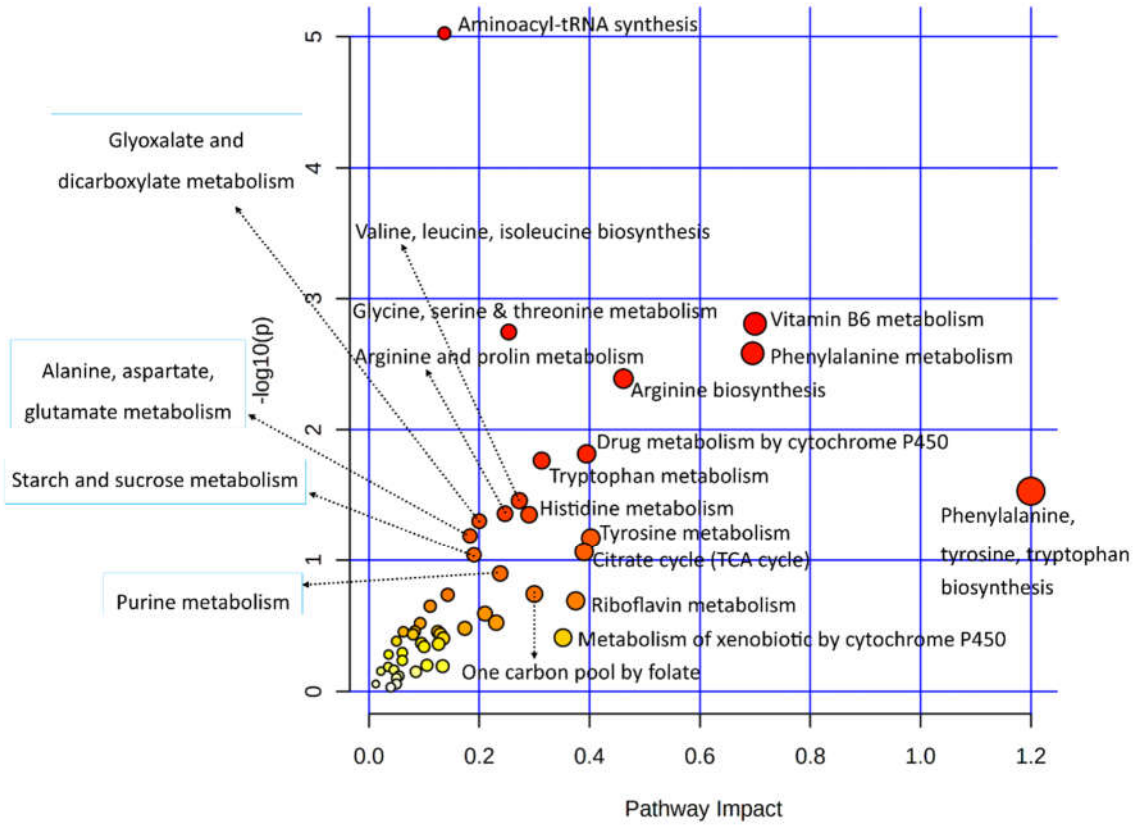

Figure 5. Dot plot illustration of metabolic pathways enrichment in joint analysis of significant differentially expressed genes and important metabolites from transcriptome and metabolome data, respectively. Various metabolic pathways with in upper and left quadrants are labelled. Size of dots increase with increasing pathway impact, while color intensifies according to y-axis.

2.4. Important pathways, metabolites and genes in joint pathways analysis

Joint analysis of metabolome and transcriptome data (under sub-section 2.2.1) was queried for significant and interesting functional pathways related to cellular functions and adaptation of granulosa cells to heat stress (Table 2).

Preprints (www.preprints.org) | NOT PEER-REVIEWED | Posted: 27 April 2022 doi:10.20944/preprints202204.0248.v1

Table 2. Important functional pathways, metabolites and genes. Important enriched pathways from integrated analysis of metabolites and genes are divided into top general functional pathways, top cell signaling and functional pathways, and cancer pathways. Complete statistical detailing of pathways, list of functional hits along with their regulation status are given.

Joint pathways	Total /Hits	Raw *P*-value	Holm adjust *P*-value	Metabolites	Genes
Top functional pathways from integrated analysis					
ABC transporters	198/18	5.11E-11	1.67E-08	↓ Alpha-Trehalose; ↓ D-Mannitol; ↑ L-Lysine; ↑ L-Arginine; ↑ L-Glutamine; ↓ L-Histidine; ↑ L-Leucine; ↓ L-Threonine; ↓ Proline; ↑ Choline; ↓ Thiamine; ↓ Ciliatine; ↓ L-Phenylalanine; ↓ Riboflavin; ↓ Uridine; ↓ Xanthosine	↓ ABCC5; ↓ ABCA2;
Protein digestion and absorption	168/11	8.70E-06	0.002819	↑ L-Leucine; ↓ L-Phenylalanine; ↓ L-Tryptophan; ↓ L-Threonine; ↑ L-Glutamine; ↑ L-Arginine; ↑ L-Lysine; ↓ L-Histidine; ↓ Proline; ↑ L-Tyrosine	↓ COL11A2
Taste transduction	112/6	0.0028879	0.91259	↓ Serotonin; ↑ Citric Acid	↓ SCN9A; ↓ PDE1A; ↓ GABBR1; ↓ GNB3
Cocaine addiction	56/4	0.0053408	1.00000	↑ L-Tyrosine;	↓ MAOB; ↓ RGS9; ↓ GRIN2D
GABAergic synapse	99/5	0.0082127	1.00000	↑ L-Glutamine; ↓ Succinic Acid	↓ GABBR1; ↓ ADCY2; ↓ GNB3
Functional signaling pathways (manual query of integrated analysis)					
cAMP signaling pathway	254/8	0.015042	1.00000	↓ Serotonin; ↓ Succinic Acid	↓ RYR2; ↓ ATP2A1; ↓ GRIN2D; ↓ GABBR1; ↓ ADCY2; ↓ OXT
Ovarian steroidogenesis	78/4	0.016783	1.00000	↓ Progesterone	↓ ADCY2; ↓ CYP1B1 ↓ PLA2G4B
mTOR signaling pathway	158/4	0.1386	1.00000	↑ L-Leucine; ↑ L-Arginine	↓ DEPTOR; ↓ WNT11
AMPK signaling pathway	146/2	0.5515	1.00000	↓ AICAR	↑ SLC2A4
Cancer pathways (manual query of integrated analysis)					
Central carbon metabolism in cancer	103/11	6.5E-08	2.1E-05	↑ L-Glutamine; ↑ Citric Acid; ↓ Succinic Acid; ↑ L-Leucine; ↓ L-Phenylalanine; ↓ L-Histidine; ↓ L-Tryptophan; ↑ L-Tyrosine; ↓ Proline; ↑ L-Arginine	↑ SLC16A3
Breast cancer	153/3	0.30314	1.00000	↓ Progesterone	↓ CSNK1B; ↓ WNT11
Prostate cancer	109/2	0.40000	1.00000	↓ Progesterone	↓ INSRR
Pathways in cancer	573/8	0.43410	1.00000	↓ Progesterone	↓ WNT11; ↓ IGF2; ↑ NOS2; ↓ VEGFA; ↓ ADCY2; ↓ GNB3; ↑ GSTA5

Preprints (www.preprints.org) | NOT PEER-REVIEWED | Posted: 27 April 2022 doi:10.20944/preprints202204.0248.v1

Furthermore, network analysis of all pathways was carried out using transcriptome and metabolome data input, Figure 6A present the comprehensive network of integrated pathways network, where all mapped queries of metabolites involved in pathways with more than 1 hits are labelled. Similarly Figure 6B shows the same network, with labelled metabolites nodes involved in multiple pathways with more than 1 hits. Complete statistical details of this integrated network analysis of all pathways and enriched genes and metabolites are presented in supplementary table S6.

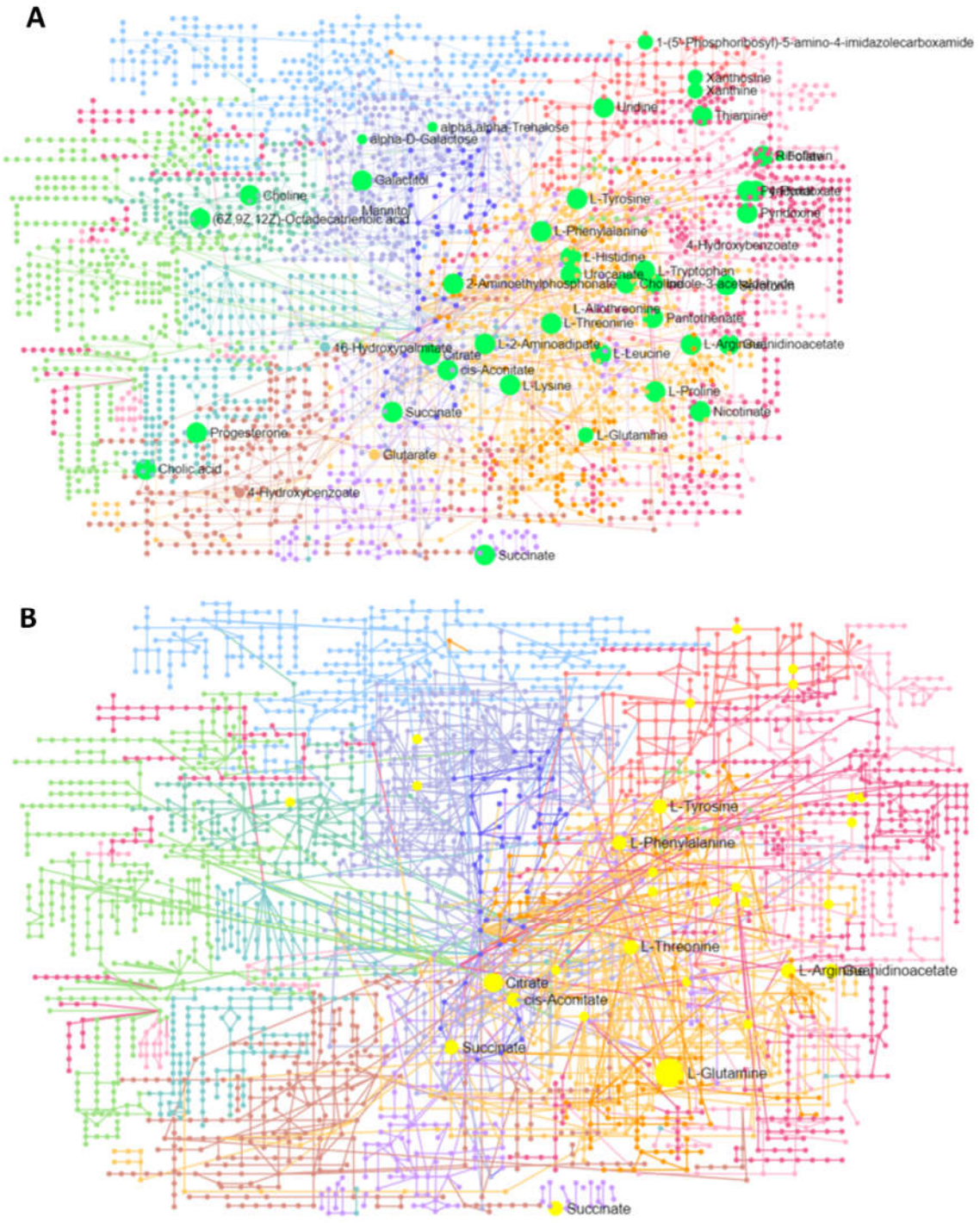

Figure 6. Network analysis of pathways carried out using integrated analysis of all pathways using transcriptome and metabolome data input, Figure 6A present the comprehensive network of integrated pathways, where all mapped queries of metabolites (highlighted in light green color) involved in pathways with more than 1 hits are labelled. Similarly Figure 6B shows the same

Preprints (www.preprints.org) | NOT PEER-REVIEWED | Posted: 27 April 2022 doi:10.20944/preprints202204.0248.v1

network, with metabolites nodes involved in multiple pathways (highlighted in yellow color) with more than 1 hits, being labelled.

Additionally, joint metabolic analysis of both transcriptome data (under sub-section 2.3.3) was queried for significant and interesting metabolic pathways related to cellular functions and adaptation of granulosa cells to heat stress (Table 3).

Table 3. Important functional pathways, metabolites and genes. Important metabolic pathways from integrated analysis of metabolites and genes are presented. Complete statistical detailing of pathways, list of functional hits along with their regulation status are given.

Metabolic pathways	Total /Hits	Raw *P*-value	Holm adjust *P*-value	Metabolites	Genes
Vitamin B6 metabolism	21/4	0.00156	0.12918	↑ Pyridoxine; ↓ Pyridoxal; ↑ 4-Pyridoxic Acid	↑ AOX1
Glycine, serine and threonine metabolism	72/7	0.00180	0.14759	↑ Choline; ↓ Glycocyamine; ↓ L-Threonine; ↑ L-Allo-Threonine;	↓ MAOB; ↓ AOC2; ↓ AMT
Phenylalanine metabolism	24/4	0.00261	0.21157	↓ L-Phenylalanine; ↑ L-Tyrosine;	↓ AOC2; ↓ MAOB
Arginine biosynthesis	27/4	0.00408	0.32625	↑ L-Arginine; ↑ L-Glutamine;	↑ NOS2; ↓ GPT
Tryptophan metabolism	84/6	0.017185	1.00000	↓ L-Tryptophan; ↓ Serotonin; ↑ Indole-3-Acetaldehyde;	↓ CYP1B1 ↓ MAOB; ↑ AOX1
Arginine and proline metabolism	78/5	0.04371	1.00000	↑ L-Arginine; ↓ Glycocyamine; ↓ Proline	↑ NOS2; ↓ MAOB
Histidine metabolism	32/3	0.04444	1.00000	↓ Urocanic Acid; ↓ L-Histidine	↓ MAOB
Glyoxylate and dicarboxylate metabolism	56/4	0.04982	1.00000	↓ Cis-Aconitic Acid; ↑ Citric Acid; ↑ L-Glutamine	↓ AMT
Alanine, aspartate and glutamate metabolism	61/4	0.06459	1.00000	↑ L-Glutamine; ↑ Citric Acid; ↓ Succinic Acid	↓ GPT
Tyrosine metabolism	88/5	0.06715	1.00000	↑ L-Tyrosine	↓ MAOB; ↑ ADH6; ↓ AOC2; ↑ AOX1
Starch and sucrose metabolism	43/3	0.09127	1.00000	↓ Alpha-Trehalose	↓ AMY2B; ↑ PYGM
Purine metabolism	169/7	0.12673	1.00000	↓ Xanthine; ↑ L-Glutamine; ↓ AICAR; ↓ Xanthosine	↓ PDE1A; ↓ ADCY2; ↓ PKLR
One carbon pool by folate	31/2	0.18155	1.00000	↑ Folic Acid	↓ AMT

2.5. Interaction network analysis among transcriptome and metabolome data

2.5.1. Interaction network analysis among genes and metabolites

Significant differentially expressed genes and metabolites were used to carry out KEGG based interactive network analysis among them, as shown in interaction network illustration in Figure 7, where important nodes are highlighted. Statistical details of joint interaction of top interactions and with those involving two or more nodes along their regulation status in respective studies are given in Table 4, while the complete statistical details of this network are given in supplementary table S6.

Preprints (www.preprints.org) | NOT PEER-REVIEWED | Posted: 27 April 2022 doi:10.20944/preprints202204.0248.v1

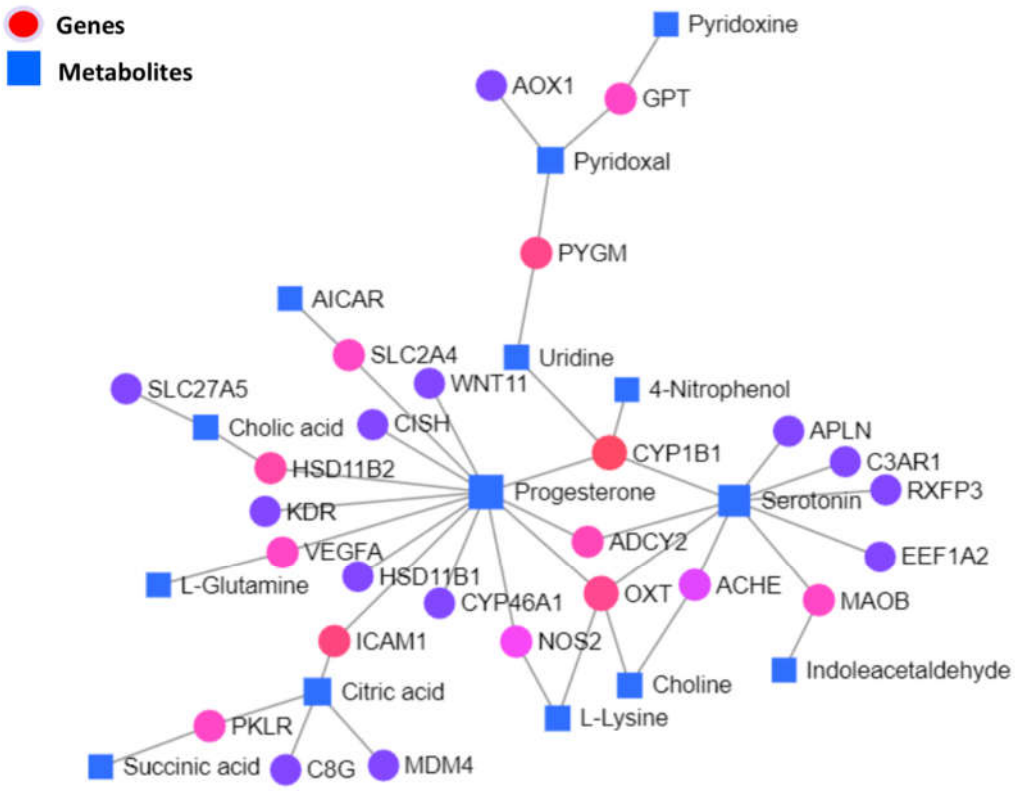

Figure 7. Integrated network illustration of differential genes and metabolites based on KEGG database. Where circular nodes represent genes, square nodes represent metabolites as labelled. Color variation of gene nodes from red to violet is based upon the degree of connections in network.

Preprints (www.preprints.org) | NOT PEER-REVIEWED | Posted: 27 April 2022 doi:10.20944/preprints202204.0248.v1

Table 4. Statistical details of top interactions nodes found in joint network analysis of genes and metabolites, along with their regulation status in heat stressed granulosa cells. "Degree" denotes the number of direct connections between nodes, "Betweeness" show the centrality of the given interaction.

Id	Label	Regulation status	Degree	Betweenness
C00410	Progesterone	Down	13	544.42
C00780	Serotonin	Down	9	254.42
1545	*CYP1B1*	Down	4	281
C00158	Citric acid	Up	4	145
5020	*OXT*	Down	4	112
C00250	Pyridoxal	Down	3	110
3383	*ICAM1*	Up	2	170
C00299	Uridine	Down	2	170
5837	*PYGM*	Up	2	140
3291	*HSD11B2*	Down	2	74
108	*ADCY2*	Down	2	51
4129	*MAOB*	Down	2	38
7422	*VEGFA*	Down	2	38
5313	*PKLR*	Down	2	38
6517	*SLC2A4*	Up	2	38
2875	*GPT*	Down	2	38
C00695	Cholic acid	Down	2	38
4843	*NOS2*	Up	2	12.5
43	*ACHE*	Down	2	6.5
C00114	Choline	Up	2	6.08
C00047	L-Lysine	Up	2	3.08

2.5.2. Interaction network among metabolites

Joint interaction network among metabolites based on KEGG database is illustrated in Figure 8. Important central metabolites as labelled in network illustration are statistically detailed along their regulation status in heat stressed granulosa cells, in Table 5. While the statistical details of the whole interaction network are given in supplementary table S6.

Preprints (www.preprints.org) | NOT PEER-REVIEWED | Posted: 27 April 2022 doi:10.20944/preprints202204.0248.v1

Figure 8. Integrated network illustration of differential metabolites based on KEGG database. Where circular nodes represent different metabolites at different degree of interaction made through line connecting and originating them. Central important metabolites in network are labelled.

Preprints (www.preprints.org) | NOT PEER-REVIEWED | Posted: 27 April 2022 doi:10.20944/preprints202204.0248.v1

Table 5. Major diseases and its directly associated metabolites and genes are listed. "Degree" denotes the number of direct connections between nodes, "Betweeness" show the centrality of the given interaction. While, the list of interaction network nodes is given against each corresponding disease along with it regulation status in heat stressed granulosa cells.

Id	Label	Regulation status	Degree	Betweenness
C00158	Citric acid	Up	131	26439.49
C00047	L-Lysine	Up	112	17872.77
C00042	Succinic acid	Down	105	20430.26
C00064	L-Glutamine	Up	105	17053.91
C00780	Serotonin	Down	101	20433.61
C00123	L-Leucine	Up	76	7023.93
C00188	L-Threonine	Down	72	5723.68
C00082	L-Tyrosine	Up	65	9222.24
C00114	Choline	Up	64	9738.79
C00148	L-Proline	Down	56	5378.26
C05519	L-Allo-threonine	Up	52	3135.83
C00299	Uridine	Down	50	9847.77
C00695	Cholic acid	Down	41	4475.47
C00250	Pyridoxal	Down	39	2385.19
C00984	D-Galactose	Down	33	6225.15

2.5.3. Interactive network analysis among genes, metabolites and diseases

Significant differentially expressed genes and metabolites were used to carry out KEGG based interactive disease network analysis, as shown in interaction network illustration in Figure 8, where important disease, genes, and metabolites nodes are highlighted. Statistical details of joint interaction of top disease interactions, metabolites and genes enriched along their regulation status are given in Table 6, while the complete statistical details of this network are given in supplementary table S6.

Preprints (www.preprints.org) | NOT PEER-REVIEWED | Posted: 27 April 2022 doi:10.20944/preprints202204.0248.v1

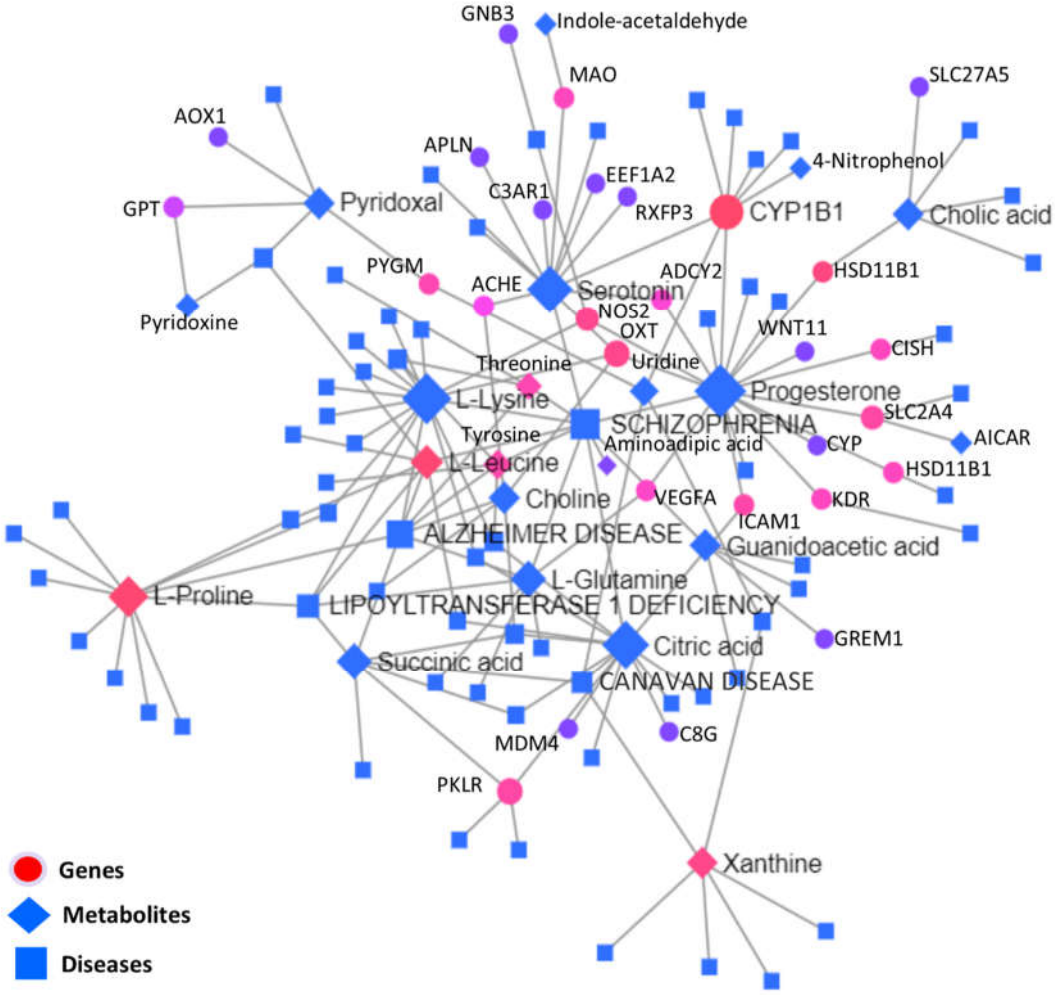

Figure 8. KEGG based interaction network analysis among metabolites, genes and diseases, where different shapes of nodes denotes different character, and lines between different nodes show connections.

Preprints (www.preprints.org) | NOT PEER-REVIEWED | Posted: 27 April 2022 doi:10.20944/preprints202204.0248.v1

Table 6. Major diseases and its directly associated metabolites and genes form network analysis are listed. "Degree" denotes the number of direct connections among nodes, "Betweeness" show the centrality of the given interaction. While, the list of interaction network nodes is given against each corresponding disease along with their regulation status in heat stressed granulosa cells.

Id	Disease	Degree	b/w	Metabolites	Genes
181500	SCHIZOPHRENIA	10	1086	↓ Progesterone, ↑ L-Lysine, ↓ Serotonin, ↑ Citric acid, ↑ L-Glutamine, ↓ Threonine, ↓ Aminoadipic acid	↓ *VEGFA*
104300	ALZHEIMER DISEASE	8	542	↑ L-Lysine, ↑ L-Leucine, ↑ L-Glutamine, ↑ Choline, ↓ L-Proline, ↓ Threonine	-
616299	LIPOYLTRANSFERASE 1 DEFICIENCY	5	286	↑ L-Lysine, ↑ L-Leucine, ↑ L-Glutamine, ↓ Succinic acid, ↓ L-Proline, ↓ Threonine	-
271900	CANAVAN DISEASE	4	453	↓ Uridine, ↓ Xanthine, ↑ Citric acid, ↓ Succinic acid	-
617290	EPILEPSY, VITAMIN B6-DEPENDENT	3	203	↓ Pyridoxal, ↑ Pyridoxine, ↑ L-Leucine	-
276700	TYROSINEMIA, TYPE I	3	56	↓ Threonine, ↑ L-Tyrosine, ↑ L-Lysine	-

b/w: betweeness; ↑ : up-regulated in heat stress; ↓ : down-regulated in heat stress

In order to get functional insights into the DEGs found in multiple integration and network analysis of transcriptome and metabolome, all of those DEGs were combined and physical protein-protein interaction (PPI) network analysis (STRING) with medium confidence score (0.4) was carried out, as presented in Figure 9. Whereas on the basis of experimentally verified, curated database interactions, and text mining, 4 subnetworks were observed. *GNB3*, *KDR*, *CYP1B1*, *ADCY2*, *RGS9*, *INSRR*, *GSTA5*, *VEGFA*, *ADH6*, *IGF2* and *MDM4* were the central network nodes.

Preprints (www.preprints.org) | NOT PEER-REVIEWED | Posted: 27 April 2022 doi:10.20944/preprints202204.0248.v1

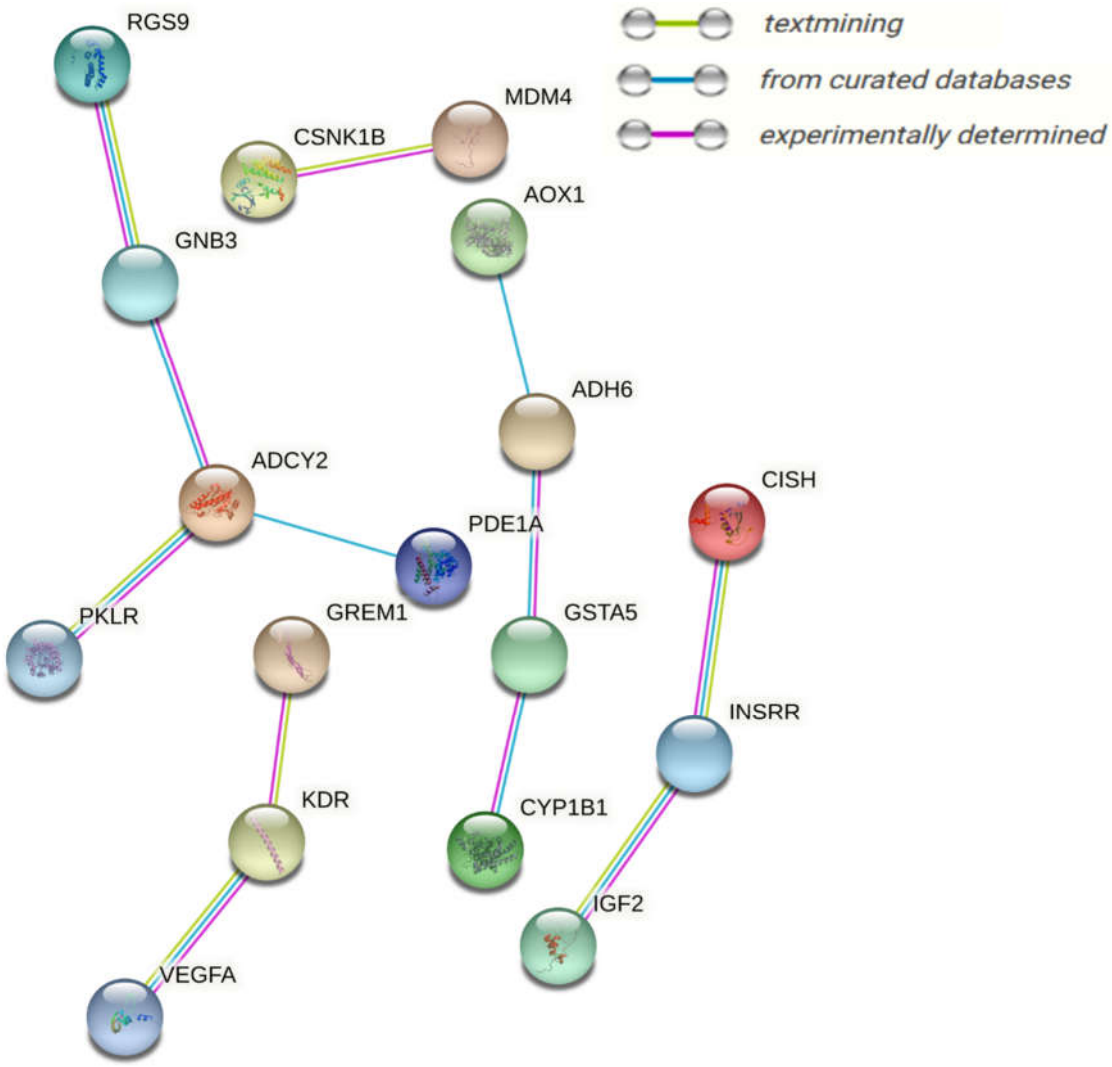

Figure 9. Differentially expressed genes found in multiple integration and network analysis of transcriptome and metabolome response of granulosa cells to acute heat stress are drawn into physical protein-protein interaction network (STRING) with medium confidence score (0.4) Nodes represent proteins and lines between nodes refer to edges showing various sorts of interactions denoted by different colors and defined through the figure legends.

3. Discussion

Heat stress caused biochemical alterations in the maternal reproductive system has been attributed to low conception rates and higher embryonic losses in cattle [12,23,24]. Granulosa cells present in the ovarian follicles are important for oocyte development due to their specialized steroidogenesis role and cross talk with oocytes [1,2]. Besides our studies [4,21], earlier studies also extensively reported the adverse effect of varying degree of heat stress on granulosa cells [3,19,25]. Where, heat stress promoted oxidative stress, inflammatory cytokine signaling, an evidence of intricate survival fight in the presence of pro-apoptotic and anti-apoptotic genes, and energetic support pathways [4,21]. This study furthers our knowledge into these complex mechanisms of survival and death.

A pronounced decline of cell proliferation potential was observed in heat stressed granulosa cells. Earlier studies also report similarly, where acute heat stressed (45 °C) granulosa cells regained proliferation by 48hrs after the completion of heat treatment [19,20,26]. However, the 48 h trend of cell proliferation activity recovery followed the results reported by other studies in granulosa cells [3,27]. Interestingly, we earlier reported that treatment group with immediate culture media change after the completion of heat stress was relatively earlier to show positive proliferation change compared to the heat stress group with culture medium change at 48 h [21]. This phenomenon need further

investigation, a preliminary hypothesis may be drawn that heat stress is an energy intensive process, as supported by our previous review of literature studies [8,28,29]. Acute heat stress accumulated intracellular ROS and caused increase in apoptosis of granulosa cells, this phenomenon is commonly observed in heat stressed cells [4,25]. Certain levels of ROS keep producing due to fundamental biological processes of cells [30]. Nevertheless, higher intracellular ROS in the presence of stress and mitochondrial damage [3] impairs cell antioxidant response elements (ARE) and causes oxidative stress [4,31]. This oxidative stress may ultimately induce granulosa cell apoptosis and compromises the optimal ovarian functions [32,33]. Stress response pathway, Nrf2 pathway is particularly involved in diverse up regulatory functions related to cell metabolism in conjunction with NF-κB (nuclear factor kappa light chain enhancer of activated B cells) [34,35], PI3K/AKT/mTOR [36–38], and AMPK signaling pathways [39]. This integration analysis of metabolome and transcriptome data indicated high amino acid metabolism pathways and metabolites, of which tyrosine, tryptophan, threonine, phenylalanine and arginine metabolism pathways are enriched, indicating implication of these pathways. Nrf2 and NF-κB pathways are supportive and sometimes antagonistic to bring up cellular homeostasis in the event of stress, while NF-κB promote inflammation and inflammation subsequently promote transcription activities related to energetic catabolic support [40]. While the complex role of the Transforming growth factor-β (TGF-β) pathway is also important in this context, which is involved in signaling mechanisms related to upregulation of NF-κB and inducing apoptosis through cell cycle arrest [41,42]. Our integration analysis supports this discussion where we did found TGF-β and VEGF signaling pathways implicated in heat stressed granulosa cells. Regarding the involvement of AMPK signaling pathway, our integration analysis provide enough evidence of it most versatile involvement, as depicted by *PYGM*, *IGF2*, *MAOB*, *INSL3*, *AOC2*, *AOX1*, *ATP2A1*, *SLC2A4*, *SLC27A5*, *ADH6*, *NOS2*, etc. These genes are particularly involved in catabolic support to heat stressed granulosa cells, as shown by starch and sucrose metabolism and various amino acid metabolism pathways.

ATP-binding cassette (ABC) transporters constitutes a superfamily of conserved membrane proteins responsible for transport of nutrients across cells [43]. This pathway is interesting due to its role in cholesterol and lipid transport [44], as earlier we reported low steroidogenic activity of heat stressed granulosa cells despite the evidence of upregulation of cholesterol synthesis in heat stressed granulosa cells [21,22]. Protein digestion and absorption pathway was the second most significant pathway enriched in integrated analysis, where leucine, glutamine, arginine and tyrosine were upregulated in heat stressed granulosa cells. Yielding of amino acids and possibly their catabolism in heat stressed granulosa cells in conjunction to high inflammatory response, upregulation of Nrf2 pathway and *SLC7A11*[45], may be a protective strategy of heat stressed granulosa cells [21,22]. Another important pathway where metabolites and genes converged is cAMP signaling pathway. Mitochondrial stress, oxidative stress and cAMP signaling pathway nexus [46] appears to be correlated in heat stressed granulosa cells [3,4]. Furthermore, cAMP signaling pathway activate complex signaling involving MAPK pathway, can ultimately promote DNA damage and cell senescence [47]. The most important integrated enrichment pathway may probably the ovarian steroidogenesis. This pathway enrichment support our earlier findings of low progesterone synthesis by heat-stressed granulosa cells [4,21]. In our integrated analysis, the enrichment of mTOR pathway is reported with 4 hits including upregulation of leucine and arginine, and downregulation of WNT11 and DEPTOR. mTOR pathway is shown to downregulate in cell cycle arrest and its duopoly with IGF2 pathway should be investigated further at metabolic and cell senescence level in heat-stressed granulosa cells [48,49]. The most interesting evidence is of AMPK signaling pathway, characterized by upregulation of GLUT4. Regarding the AMPK signaling pathway in our transcriptomic study [21], it is characterized by down regulation of ATP genes family and *PPARGC1A*, and upregulation of *SIRIT1, SLC2A4, HMGCS1*, and *SERBP1* [39,50]. Glutamine and citric acid, both upregulated metabolites, were found as the most abundantly enriched metabolite nodes

 doi:10.20944/preprints202204.0248.v1

in integrated interaction network analysis of both omics data. These both metabolites were enriched in many pathways, and appears as the most important markers of the heat stressed phenotype of granulosa cells.

Joint network analysis of metabolites and genes revealed *CYP1B1*, *PYGM*, *ICAM1*, *HSD11B2*, and *OXT*. Downregulation of *HSD11B2* is justifiable as the evidence of low steroidogenic capacity of heat stressed granulosa cells [4,21], however we had additional strong evidence of transcriptional suppression of steroidogenic potential of heat stressed granulosa cells in the form of genes observed in integrated analysis, like, *ADCY2*, *CYP1B1*, *PLA2G4B*. This decline of steroidogenic activity of GCs can be attributed to the transcriptional downregulation of *STAR*, *CYP11A1* [4] and mitochondrial damage due to ROS [3]. This study could not grab deep mechanisms regarding steroidogenesis modulation in heat stressed granulosa cells, however, our results presents with further line of investigation. The established phenomenon of blunt non esterified fatty acids response in heat stressed cows is characterized by low fats mobilization [11,51,52]; upregulated genes involved in fatty acids and cholesterol metabolism indicates that fatty acid metabolism is an adaptation of heat stressed granulosa cells. It can be concluded that fats mobilization is altered at organism level in heat stress, but cellular metabolism of fats remains enhanced. Therefore, supplemental fats can help to avert the heat stressed typical negative energy balance and associated adverse effects [53]. Furthermore, upregulated *ICAM1* and *PYGM* are probably the interesting findings. Amino acid catabolism and altered immune response in shape of upregulated cytokine signaling may explain its role in heat stressed granulosa cells adaptation and cancer cells. Highly upregulated *PYGM* gene, an enzyme involved in glycogenolysis, is involved in diverse insulin and glucagon signaling, necroptosis, inflammatory response, cellular energy support and cancer progression [54]. Similarly, upregulated *ICAM1* in one carbon metabolism pathway through integrated analysis, is an important finding because its upregulation reduces ovarian cancer cell growth [55]. And at the same time need further investigation because our transcriptome data suggested high inflammatory response, in the form of upregulated TLRs, cytokines, Fas and Fasl [55].

Four cancer pathways enrichment was observed in this study, characterized by upregulation of glutamine, citric acid, leucine, arginine, tyrosine and downregulation of progesterone. These findings are very related to cancer, as heat stressed cells resembles the cancer phenotype and at the same time heat treatment is a potential therapy for treatment of tumors. Heat treatment is long regarded as an important treatment option for cancer [56], however, there cons of heat treatment too, like studies reporting multipolar divisions in cancer cells, ultimately facilitating tumor heterogeneity [57]. An interplay of energy metabolic dynamism is reported in hyperthermia-resistant ovarian cancer cells [58]. Metabolic changes are shown to play decisive role in the heat treatment based cell death [59]. The most important gene found in cancer pathways through integrated analysis is s *SLC16A3*, a monocarboxylate transporter [60]. This gene involved in energetic metabolism through fatty acids metabolism and connected role in citrate cycle [60], is complicated in cancer through p53 and mTOR pathway [60,61]. While the upregulated status of *SLC16A3* is particularly shown as prognostic biomarker of cancer aversion [60,61], its upregulation in heat-stressed granulosa cells notable. While too little apoptosis in cell senescence scenario causes malignancy in cells, apoptosis pathways are complex and problem at any step can hinder cancer treatment, still targeting for apoptosis will remain main cancer treatment strategies [62]. In this integration analysis we observed *MDM4* and *CSNK1B* being interconnected and nodes towards the involvement of p53 signaling pathway at the conjunction of metabolic pathways through complex transcription mechanisms. Our transcriptomics study reporting upregulation of p21, p16, and downregulation of p53 is interesting, suggesting cell cycle arrest in heat stressed granulosa cells [21], and may lead to cellular senescence phenotype [63]. In the absence of p53 and associated *MDM4* activity, and upregulated p21 and p16, a fight between cell senescence and apoptosis can be assumed [63–65]. Senescent cells remain viable, alters metabolic and gene expression profile [63]. Metabolic alterations related to Acetyl-CoA,

 doi:10.20944/preprints202204.0248.v1

citrate cycle, and amino acid catabolism are evident in our metabolome data of heat treated granulosa cells [22]. Recently, dysregulation of amino acids like tryptophan, phenylalanine and tyrosine are implicated in colorectal cancer [66]. Cell cycle arrest can also induce cell apoptosis, where along with co-expression of p21 and p16, p53 appears as a double edged sword [67]. Heat stress is shown to alter the morphology of granulosa cells [19], upregulate DNA damage and genes related to structural remodeling [3,21]. These phenomena ultimately can lead to activation of p53, inducing cell-cycle arrest, apoptosis, senescence and DNA repair [68,69]. High ROS activity, downregulated *MDM4*, *IGF2*, *PPARGC1A*, *PPARGC1B*, and upregulated *HIF1A* suggests interconnecting role of p53 and heat stressed mitochondrial damage [68,70], as shown in an in-vitro heat stress treatment study in mammary epithelial cells [71].

4. Methods

4.1. Granulosa Cell Culture, Heat Treatment and Cell experiments

Cell collection, culture and treatment methods followed our previous study [21,22,72]. In brief, follicular fluid was collected from small follicles (3–8 mm) of cyclic bovine ovaries followed by filtration, centrifugal washings. Obtained cells were seeded on coverslips in a 12-well plate DMEM/F12 medium containing 10% FBS (both from Thermo Fisher Scientific, Waltham, MA, USA). After 24 h culturing, cells were fixed, permeabalized, washed with PBS, loaded with 5% goat serum for 1 h, and incubated with FSHR antibody (1:1500, Sigma Aldrich, St. Louis, MI, USA) at 4 °C for overnight. In the next step, cells were subjected to FITC-conjugated secondary antibody for 2 h, followed by washing and PI staining (Nanjing Jiancheng Bio Inst., Nanjing, China). Finally, slides were observed under a fluorescence microscope (Olympus, Tokyo, Japan). The obtained granulosa cells were initially cultured for 48 h and subsequently subjected to 2 h of acute heat stress (43 °C versus 38 °C).

Reactive oxygen species, apoptosis and hormone measurement methods followed our previous studies [21,22,72]. Cells were cultured at the rate of 2×10^4 for colorimetric CCK-8 and 1×10^4 in each well of 96-well plates for fluorocolorimetric ROS assay (DCFDA kit, Abcam, Cambridge, MA, USA). Post-treatment absorbance of cells was measured at a 450 nm wavelength by a plate reader, followed by measurements at various time intervals. The qualitative apoptosis rate of cells was measured by through fluorescence microscope (Axio Imager A2; ZEISS Microscopy, Oberkochen, BW, Germany) with an Annexin V-FITC kit (Nanjing Jiancheng Bio Inst., Nanjing, China). Similarly, determination of P4 and E2 concentration in treated cells culture media was measured according to the manufacturer's protocols of respective ELISA kits (Cusabio Technology LLC, Wuhan, Hubei, China). The data from at least six replicates each for cell proliferation, ROS, apoptosis measurements and ELISA were analyzed using Graphpad Prism version 9.0.0 for windows (GraphPad Software, Inc. San Diego, California USA). Analysis of variance was carried out and means were compared through Tukey's honestly significant difference (HSD) test at a 5% level of significance ($\alpha = 0.05$). All the data presented in the figures are expressed as mean ± standard error (S.E).

4.2. Transcriptomics data and differentially expressed genes

Comprehensive methods of RNA sequencing are explained in our previous articles [21,22]. In brief, the RNA was isolated from control (38 °C) and heat stressed (43 °C for 2 h) bovine granulosa cells according to the TRIzol Reagent method [39]. RNA quality, integrity, and concentration were assessed, followed by the cDNA library with the NEBNext Ultra RNA Library Prep Kit for Illumina (Cat No. E7530S, New England Biolabs (UK) Ltd., Hitchin, Herts, UK) and finally submitted for sequencing by the NovaSeq 6000 System (Illumina, Inc., San Diego, CA, USA), which generated 150 base paired-end reads. The quality check (FastQC software (v0.11.9) and global trimming (Fastp, v0.20.0) [73], reads were mapped to the bovine genome of version ARS-UCD1.2. Gene expression counts were investigated through RNA-SeQC software (v2.3.6) [73]. PCA and clustering structure were performed using the psych and hcluster R packages. For DEGs screening,

 doi:10.20944/preprints202204.0248.v1

the quantile-adjusted conditional maximum likelihood (qCML) was performed using edgeR in the R package [74] with criteria fold change ≥ 1.5 and 0.05 for the alpha of false discovery rate (FDR). Finally, 330 significant DEGs were determined in control versus heat stressed bovine granulosa cells groups comparison.

4.3. Metabolomics data and differentially expressed metabolites

Comprehensive methods involved in metabolome assay are detailed in our previous study [22]. Briefly, cell culture fluid was collected for control (38 °C) and heat stress (43 °C for 2 h) groups after treatment. After initial methanol extraction, 3 replicate samples from each group were dispatched for liquid chromatography-tandem mass spectrometry (LC-MS/MS) analysis. Further, metabolites extraction was done through ice-cold acetonitrile, samples were air dried and re-suspended in pure water. All extracted samples and quality controls were run through LC-MS/MS using HSS T3 100 * 2.1 mm 1.8 μm column (Waters) on Ultimate 3000 (Thermo Fisher Scientific, Waltham, MA, USA) followed by the analysis employing Q Exactive system (Thermo Fisher Scientific, Waltham, MA, USA). Qualitative results of samples and peak intensities in both ion modes of LCMS analysis were obtained and the MSBank and KEGG databases were queried for metabolites identification. The MetaboAnalyst 5.0 package [75] was employed to carry out the PCA for investigating the clustering trends and outliers. Moreover, metabolites with Variable Importance in the Projection (VIP) values greater than 1 with their fold change values, calculated through PLS-DA, were considered as the differential metabolites between control and heat stress groups. Finally, 56 important differential metabolites list was determined in control versus heat stressed bovine granulosa cells groups comparison.

4.4. Integrated pathway analysis of genes and metabolites

Henceforth, this study did joint integration analysis of our previous metabolome [22] and transcriptome data from in-vitro acute heat stressed (43 °C for 2 h) bovine granulosa cells. Both of those earlier omics studies involved same samples and replicates. Out of 330 significant differentially expressed genes (FC ≥ 1.5 and 0.05 for the alpha of FDR), total 256 genes (along with their log2(FC) values) finally get mapped to the different KEGG databases used by the latest version of software MetaboAnalyst 5.0 [75]. Similarly, 56 important metabolites list (PLSDA, VIP score ≥ 1) along with their log2(FC) values finally get used in joint integration analysis of metabolomics and transcriptomic data in MetaboAnalyst 5.0 software [75]. In the first step of analysis, "Joint-Pathway Analysis" module of MetaboAnalyst 5.0, based on KEGG global metabolic network (ko01100), was used. Mapping of both gene and metabolite features were assessed and manually corrected in case of matching options available. First step of analysis involved following sub-modules, "All pathways (gene only)", "Metabolic pathways (metabolites only)", "All pathways (integrated)", and "Metabolic pathways integrated". Default settings were maintained as, enrichment analysis based on "Hypergeometric test"; topology measure as "Degree centrality"; integration method of "Combined queries". Dot plots, tables of pathway results and matched features were saved and downloaded for each analysis. Additionally, module of "All pathways (integrated)" was also used for visualization of network among pathways and enriched features.

4.5. Interaction network analysis among genes and metabolites

For this purpose, "Joint-Pathway Analysis" module of MetaboAnalyst 5.0 was used. Mapping of both gene and metabolite features were assessed and manually corrected in case of matching options available. In the first step, "Gene-metabolite interaction network" sub-module with default settings was used for the interaction analysis among genes and metabolites. In the second step, "Metabolite-metabolite interaction network" sub-module with default settings was used for the interaction analysis among metabolites based on both genes and metabolites data input. For third interactive network analysis, "Metabolite-gene-disease interaction network" sub-module with default settings was used for the interaction analysis among genes. Moreover, all of the important DEGs found

in the integration and network analyses of metabolome and transcriptome data were subjected to PPI physical network analysis at medium confidence score of 0.4 using STRING version 11.5 (https://cn.string-db.org/).

5. Conclusions:

The etiology of various changes in heat stressed granulosa can be at least in part attributed to varying degree of cellular stress, impairment in lipid transport and metabolism, inflammation-metabolism nexus, and disruption in energetic metabolism. Threonine, phenylalanine, and proline appeared to be the only downregulated abundant amino acids in various pathways. Similarly, involvement of downregulated succinic acid, vitamin B6, and Riboflavin in many pathways are also important and nodes towards the simple sugars and vitamins importance in fight against heat stress at cellular level. Since we observed cell proliferation activity recovery after heat stress, upregulated choline and citric acid metabolites may primarily be considered important metabolites involved in heat stressed granulosa cells. Downregulated *MAOB*, *AOC2* and upregulated *AOX1*, *ADH6* pairs involved in vitamin B6 and amino acids metabolism may be considered important candidate genes. This study provided additional evidence of transcriptional suppression of steroidogenic potential of heat stressed granulosa cells in the form of *ADCY2*, *CYP1B1*, and *PLA2G4B*, while *COL11A2* (downregulated gene) may be considered as universal candidate gene involved in the amino acid metabolism. Furthermore, upregulated *ICAM1* and *PYGM* are also probably the interesting findings regarding the inflammation metabolism nexus in granulosa cells exposed to heat stress. Besides, the demonstration of various cell signaling and metabolic pathways, this integration analysis of metabolome and transcriptome acute heat stressed granulosa cell provided an interesting conjecture of metabolites and genes through integrated analysis of transcriptome and metabolome data.

Supplementary materials: This manuscript draft has two supplementary figure (S1 and S2) and six supplementary tables from S1 to S6.

Author Contributions: A.S carried out experimentation, analysis, and writing. H.L, L.H, and A.K helped in analysis and writing. Y.W and H.Z were involved in the conception, review, supervision of the project and validation of the manuscript. All authors approved the final version and consented to publication.

Funding: This work was possible due to the financial assistance from the following projects; China Agriculture Research System of MOF and MARA, the Program for Changjiang Scholar and Innovation Research Team in University (IRT–15R62).

Data Availability Statement: All the pertinent data including that of RNA-seq and Metabolomics is already reported or presented in the manuscript and associated supplementary files.

Conflicts of Interest: Authors declare no conflict of interests. Funders had no role in the design of the study; in the collection, analyses, or interpretation of data; in the writing of the manuscript, or in the decision to publish.

References

1. Jahromi, B.N.; Mosallanezhad, Z.; Matloob, N.; Davari, M.; Ghobadifar, M.A. The potential role of granulosa cells in the maturation rate of immature human oocytes and embryo development: A co-culture study. *Clin. Exp. Reprod. Med.* **2015**, *42*, doi:10.5653/cerm.2015.42.3.111.

2. Diaz, F.J.; Wigglesworth, K.; Eppig, J.J. Oocytes determine cumulus cell lineage in mouse ovarian follicles. *J. Cell Sci.* **2007**, *120*, doi:10.1242/jcs.000968.

3. Alemu, T.W.; Pandey, H.O.; Salilew Wondim, D.; Gebremedhn, S.; Neuhof, C.; Tholen, E.; Holker, M.; Schellander, K.; Tesfaye, D. Oxidative and endoplasmic reticulum stress defense mechanisms of bovine granulosa cells exposed to heat stress. *Theriogenology* **2018**, *110*, doi:10.1016/j.theriogenology.2017.12.042.

4. Khan, A.; Dou, J.; Wang, Y.; Jiang, X.; Khan, M.Z.; Luo, H.; Usman, T.; Zhu, H. Evaluation of heat stress effects on cellular and transcriptional adaptation of bovine granulosa cells. *J. Anim. Sci. Biotechnol. 2020 111* **2020**, *11*, 1–20, doi:10.1186/S40104-019-0408-8.

5. Liu, H.L.; Liu, D.; Ding, G.R.; Liao, P.F.; Zhang, J.W. Hypoxia-inducible factor-1α and Wnt/β-catenin signaling pathways promote the invasion of hypoxic gastric cancer cells. *Mol. Med. Rep.* **2015**, *12*, doi:10.3892/mmr.2015.3812.

6. Roth, Z. Heat stress reduces maturation and developmental capacity in bovine oocytes. *Reprod. Fertil. Dev.* **2021**, *33*, doi:10.1071/RD20213.

7. Roth, Z.; Meiden, R.; Braw-Tal, R.; Wolfenson, D. Immediate and delayed effects of heat stress on follicular development and its association with plasma FSH and inhibin concentration in cows. *J. Reprod. Fertil.* **2000**, *120*, doi:10.1530/jrf.0.1200083.

8. Sammad, A.; Khan, M.Z.; Abbas, Z.; Hu, L.; Ullah, Q.; Wang, Y.; Zhu, H.; Wang, Y. Major Nutritional Metabolic Alterations Influencing the Reproductive System of Postpartum Dairy Cows. *Metab. 2022, Vol. 12, Page 60* **2022**, *12*, 60, doi:10.3390/METABO12010060.

9. Gaskins, A.J.; Mínguez-Alarcón, L.; VoPham, T.; Hart, J.E.; Chavarro, J.E.; Schwartz, J.; Souter, I.; Laden, F. Impact of ambient temperature on ovarian reserve. *Fertil. Steril.* **2021**, *116*, doi:10.1016/j.fertnstert.2021.05.091.

10. Bridges, P.J.; Brusie, M.A.; Fortune, J.E. Elevated temperature (heat stress) in vitro reduces androstenedione and estradiol and increases progesterone secretion by follicular cells from bovine dominant follicles. *Domest. Anim. Endocrinol.* **2005**, *29*, 508–522, doi:10.1016/J.DOMANIEND.2005.02.017.

11. Baumgard, L.H.; Wheelock, J.B.; Sanders, S.R.; Moore, C.E.; Green, H.B.; Waldron, M.R.; Rhoads, R.P. Postabsorptive carbohydrate adaptations to heat stress and monensin supplementation in lactating Holstein cows1. *J. Dairy Sci.* **2011**, *94*, 5620–5633, doi:10.3168/jds.2011-4462.

12. Sammad, A.; Umer, S.; Shi, R.; Zhu, H.; Zhao, X.; Wang, Y. Dairy cow reproduction under the influence of heat stress. *J. Anim. Physiol. Anim. Nutr. (Berl).* **2020**, *104*, doi:10.1111/jpn.13257.

13. Shin, E.K.; Jeong, J.K.; Choi, I.S.; Kang, H.G.; Hur, T.Y.; Jung, Y.H.; Kim, I.H. Relationships among ketosis, serum metabolites, body condition, and reproductive outcomes in dairy cows. *Theriogenology* **2015**, *84*, doi:10.1016/j.theriogenology.2015.03.014.

14. Leroy, J.L.M.R.; Vanholder, T.; Mateusen, B.; Christophe, A.; Opsomer, G.; de Kruif, A.; Genicot, G.; Van Soom, A. Non-esterified fatty acids in follicular fluid of dairy cows and their effect on developmental capacity of bovine oocytes in vitro. *Reproduction* **2005**, *130*, doi:10.1530/rep.1.00735.

15. Bromfield, J.J.; Sheldon, I.M. Lipopolysaccharide initiates inflammation in bovine granulosa cells via the TLR4 pathway and perturbs oocyte meiotic progression in vitro. *Endocrinology* **2011**, *152*, doi:10.1210/en.2011-1124.

16. Shehab-El-Deen, M.A.M.M.; Leroy, J.L.M.R.; Fadel, M.S.; Saleh, S.Y.A.; Maes, D.; Van Soom, A. Biochemical changes in the follicular fluid of the dominant follicle of high producing dairy cows exposed to heat stress early post-partum. *Anim. Reprod. Sci.* **2010**, *117*, doi:10.1016/j.anireprosci.2009.04.013.

17. Paes, V.M.; Vieira, L.A.; Correia, H.H.V.; Sa, N.A.R.; Moura, A.A.A.; Sales, A.D.; Rodrigues, A.P.R.; Magalhães-Padilha, D.M.; Santos, F.W.; Apgar, G.A.; et al. Effect of heat stress on the survival and development of in vitro cultured bovine preantral follicles and on in vitro maturation of cumulus–oocyte complex. *Theriogenology* **2016**, *86*, 994–1003, doi:10.1016/J.THERIOGENOLOGY.2016.03.027.

18. Vanholder, T.; Leroy, J.L.M.R.; Van Soom, A.; Opsomer, G.; Maes, D.; Coryn, M.; De Kruif, A. Effect of non-esterified fatty acids on bovine granulosa cell steroidogenesis and proliferation in vitro. *Anim. Reprod. Sci.* **2005**, *87*, doi:10.1016/j.anireprosci.2004.09.006.

19. Saadeldin, I.M.; Swelum, A.A.A.; Elsafadi, M.; Mahmood, A.; Osama, A.; Shikshaky, H.; Alfayez, M.; Alowaimer, A.N.; Magdeldin, S. Thermotolerance and plasticity of camel somatic cells exposed to acute and chronic heat stress. *J. Adv. Res.* **2020**, *22*, 105–118, doi:10.1016/J.JARE.2019.11.009.

20. Saadeldin, I.M.; Swelum, A.A.A.; Elsafadi, M.; Mahmood, A.; Alfayez, M.; Alowaimer, A.N. Differences between the tolerance of camel oocytes and cumulus cells to acute and chronic hyperthermia. *J. Therm. Biol.* **2018**, *74*, 47–54, doi:10.1016/J.JTHERBIO.2018.03.014.

21. Sammad, A.; Luo, H.; Hu, L.; Zhu, H.; Wang, Y. Transcriptomics Reveals Granulosa Cell's Coping through Redox, Inflammatory, Metabolic and Cytoskeleton Mechanisms under Acute Heat Stress. **2022**, doi:10.20944/PREPRINTS202202.0357.V1.

22. Sammad, A.; Hu, L.; Luo, H.; Abbas, Z.; Umer, S.; Zhao, S.; Xu, Q.; Khan, A.; Wang, Y.; Zhu, H.; et al. Investigation of Metabolome Underlying the Biological Mechanisms of Acute Heat Stressed Granulosa Cells. *Int. J. Mol. Sci. 2022, Vol. 23, Page 2146* **2022**, *23*, 2146, doi:10.3390/IJMS23042146.

23. Hansen, P.J. Embryonic mortality in cattle from the embryo's perspective. *J. Anim. Sci.* **2002**, *80*, doi:10.2527/animalsci2002.80e-suppl_2e33x.

24. Destaw, W.M.; Kefyalew, A.W. Evaluation of the reproductive performance of Holstein Friesian dairy cows in Alage ATVET college, Ethiopia. *Int. J. Livest. Prod.* **2018**, *9*, 131–139, doi:10.5897/IJLP2018.0469.

25. Wang, Y.; Yang, C.; Elsheikh, N.A.H.; Li, C.; Yang, F.; Wang, G.; Li, L. HO-1 reduces heat stress-induced apoptosis in bovine granulosa cells by suppressing oxidative stress. *Aging (Albany. NY).* **2019**, *11*, doi:10.18632/aging.102136.

26. Fu, Y.; He, C.-J.; Ji, P.-Y.; Zhuo, Z.-Y.; Tian, X.-Z.; Wang, F.; Tan, D.-X.; Liu, G.-S. Effects of Melatonin on the Proliferation and Apoptosis of Sheep Granulosa Cells under Thermal Stress. *Int. J. Mol. Sci. 2014, Vol. 15, Pages 21090-21104* **2014**, *15*, 21090–21104, doi:10.3390/IJMS151121090.

27. Fu, Y.; He, C.-J.; Ji, P.-Y.; Zhuo, Z.-Y.; Tian, X.-Z.; Wang, F.; Tan, D.-X.; Liu, G.-S. Effects of Melatonin on the Proliferation and Apoptosis of Sheep Granulosa Cells under Thermal Stress. *Int. J. Mol. Sci. 2014, Vol. 15, Pages 21090-21104* **2014**, *15*, 21090–21104, doi:10.3390/IJMS151121090.

28. Abbas, Z.; Sammad, A.; Hu, L.; Fang, H.; Xu, Q.; Wang, Y. Glucose metabolism and dynamics of facilitative glucose transporters (Gluts) under the influence of heat stress in dairy cattle. *Metabolites* **2020**, *10*, doi:10.3390/metabo10080312.

29. Sammad, A.; Wang, Y.J.; Umer, S.; Lirong, H.; Khan, I.; Khan, A.; Ahmad, B.; Wang, Y. Nutritional Physiology and Biochemistry of Dairy Cattle under the Influence of Heat Stress: Consequences and Opportunities. *Animals* **2020**, *10*, 793, doi:10.3390/ani10050793.

30. Soto, P.; Smith, L.C. BH4 peptide derived from Bcl-xL and Bax-inhibitor peptide suppresses apoptotic mitochondrial changes in heat stressed bovine oocytes. *Mol. Reprod. Dev.* **2009**, *76*, doi:10.1002/mrd.20986.

31. Abdelnour, S.A.; Abd El-Hack, M.E.; Khafaga, A.F.; Arif, M.; Taha, A.E.; Noreldin, A.E. Stress biomarkers and proteomics alteration to thermal stress in ruminants: A review. *J. Therm. Biol.* 2019, *79*.

32. Guérin, P.; El Mouatassim, S.; Ménézo, Y. Oxidative stress and protection against reactive oxygen species in the pre-implantation embryo and its surroundings. *Hum. Reprod. Update* 2001, *7*.

33. Zhang, X.-Y.; Xiong, Y.-M.; Tan, Y.-J.; Wang, L.; Li, R.; Zhang, Y.; Liu, X.-M.; Lin, X.-H.; Jin, L.; Hu, Y.-T.; et al. Melatonin rescues impaired penetration ability of human spermatozoa induced by mitochondrial dysfunction. *Reproduction* **2019**, *158*, 465–475, doi:10.1530/REP-19-0231.

34. Pedruzzi, L.M.; Stockler-Pinto, M.B.; Leite, M.; Mafra, D. Nrf2–keap1 system versus NF-κB: The good and the evil in chronic kidney disease? *Biochimie* **2012**, *94*, 2461–2466, doi:10.1016/J.BIOCHI.2012.07.015.

35. Wardyn, J.D.; Ponsford, A.H.; Sanderson, C.M. Dissecting molecular cross-talk between Nrf2 and NF-κB response pathways. *Biochem. Soc. Trans.* **2015**, *43*, 621–626, doi:10.1042/BST20150014.

36. Ganesan, S.; Summers, C.M.; Pearce, S.C.; Gabler, N.K.; Valentine, R.J.; Baumgard, L.H.; Rhoads, R.P.; Selsby, J.T. Short-term heat stress altered metabolism and insulin signaling in skeletal muscle. *J. Anim. Sci.* **2018**, *96*, doi:10.1093/jas/skx083.

37. Hambright, H.G.; Meng, P.; Kumar, A.P.; Ghosh, R. Inhibition of PI3K/AKT/mTOR axis disrupts oxidative stress-mediated survival of melanoma cells. *Oncotarget* **2015**, *6*, doi:10.18632/oncotarget.3131.

38. Reddy, N.M.; Potteti, H.R.; Vegiraju, S.; Chen, H.J.; Tamatam, C.M.; Reddy, S.P. PI3K-AKT Signaling via Nrf2 Protects against Hyperoxia-Induced Acute Lung Injury, but Promotes Inflammation Post-Injury Independent of Nrf2 in Mice. *PLoS One* **2015**, *10*, e0129676, doi:10.1371/JOURNAL.PONE.0129676.

39. Cantó, C.; Auwerx, J. PGC-1α, SIRT1 and AMPK, an energy sensing network that controls energy expenditure. *Curr. Opin. Lipidol.* **2009**, *20*, 98–105, doi:10.1097/MOL.0B013E328328D0A4.

40. He, F.; Ru, X.; Wen, T. NRF2, a Transcription Factor for Stress Response and Beyond. *Int. J. Mol. Sci. 2020, Vol. 21, Page 4777* **2020**, *21*, 4777, doi:10.3390/IJMS21134777.

41. Li, Z.Y.; Chen, Z.L.; Zhang, T.; Wei, C.; Shi, W.Y. TGF-β and NF-κB signaling pathway crosstalk potentiates corneal epithelial senescence through an RNA stress response. *Aging (Albany. NY).* **2016**, *8*, doi:10.18632/aging.101050.

42. Tominaga, K.; Suzuki, H.I. TGF-β signaling in cellular senescence and aging-related pathology. *Int. J. Mol. Sci.* 2019, *20*.

43. Rees, D.C.; Johnson, E.; Lewinson, O. ABC transporters: The power to change. *Nat. Rev. Mol. Cell Biol.* 2009, *10*.

44. Dean, M.; Annilo, T. Evolution of the ATP-binding cassette (ABC) transporter superfamily in vertebrates. *Annu. Rev. Genomics Hum. Genet.* 2005, *6*.

45. He, F.; Antonucci, L.; Karin, M. NRF2 as a regulator of cell metabolism and inflammation in cancer. *Carcinogenesis* **2020**, *41*, doi:10.1093/carcin/bgaa039.

46. Signorile, A.; Ferretta, A.; Ruggieri, M.; Paolicelli, D.; Lattanzio, P.; Trojano, M.; Rasmo, D. De Mitochondria, oxidative stress, camp signalling and apoptosis: A crossroads in lymphocytes of multiple sclerosis, a possible role of nutraceutics. *Antioxidants* 2021, *10*.

47. Lian, J.; Yue, Y.; Yu, W.; Zhang, Y. Immunosenescence: a key player in cancer development. *J. Hematol. Oncol.* 2020, *13*.

48. Blagosklonny, M. V. Cell cycle arrest is not yet senescence, which is not just cell cycle arrest: Terminology for TOR-driven aging. *Aging (Albany. NY).* **2012**, *4*, doi:10.18632/aging.100443.

49. Feng, Z.; Levine, A.J. The regulation of energy metabolism and the IGF-1/mTOR pathways by the p53 protein. *Trends Cell Biol.* 2010, *20*.

50. Mihaylova, M.M.; Shaw, R.J. The AMP-activated protein kinase (AMPK) signaling pathway coordinates cell growth, autophagy, & metabolism. *Nat. Cell Biol.* **2011**, *13*.

51. Rhoads, M.L.; Rhoads, R.P.; VanBaale, M.J.; Collier, R.J.; Sanders, S.R.; Weber, W.J.; Crooker, B.A.; Baumgard, L.H. Effects of heat stress and plane of nutrition on lactating Holstein cows: I. Production, metabolism, and aspects of circulating somatotropin. *J. Dairy Sci.* **2009**, *92*, 1986–1997, doi:10.3168/jds.2008-1641.

52. Sammad, A.; Wang, Y.J.; Umer, S.; Lirong, H.; Khan, I.; Khan, A.; Ahmad, B.; Wang, Y. Nutritional physiology and biochemistry of dairy cattle under the influence of heat stress: Consequences and opportunities. *Animals* 2020, *10*.

53. Wang, J.P.; Bu, D.P.; Wang, J.Q.; Huo, X.K.; Guo, T.J.; Wei, H.Y.; Zhou, L.Y.; Rastani, R.R.; Baumgard, L.H.; Li, F.D. Effect of saturated fatty acid supplementation on production and metabolism indices in heat-stressed mid-lactation dairy cows. *J. Dairy Sci.* **2010**, *93*, 4121–4127, doi:10.3168/JDS.2009-2635.

54. Migocka-Patrzałek, M.; Elias, M. Muscle glycogen phosphorylase and its functional partners in health and disease. *Cells* **2021**, *10*, doi:10.3390/cells10040883.

55. De Groote, M.L.; Kazemier, H.G.; Huisman, C.; Van Der Gun, B.T.F.; Faas, M.M.; Rots, M.G. Upregulation of endogenous ICAM-1 reduces ovarian cancer cell growth in the absence of immune cells. *Int. J. Cancer* **2014**, *134*, doi:10.1002/ijc.28375.

56. DeNardo, G.L.; DeNardo, S.J. Update: Turning the Heat on Cancer. *https://home.liebertpub.com/cbr* **2009**, *23*, 671–679, doi:10.1089/CBR.2008.0591.

57. Chen; Liu; Huang; Li; Zhao; Feng; Zhao Heat Stress-Induced Multiple Multipolar Divisions of Human Cancer Cells. *Cells* **2019**, *8*, doi:10.3390/cells8080888.

58. Kanamori, T.; Miyazaki, N.; Aoki, S.; Ito, K.; Hisaka, A.; Hatakeyama, H. Investigation of energy metabolic dynamism in hyperthermia-resistant ovarian and uterine cancer cells under heat stress. *Sci. Rep.* **2021**, *11*, doi:10.1038/s41598-021-94031-9.

59. Xie, S.; Sun, W.; Zhang, C.; Dong, B.; Yang, J.; Hou, M.; Xiong, L.; Cai, B.; Liu, X.; Xue, W. Metabolic Control by Heat Stress Determining Cell Fate to Ferroptosis for Effective Cancer Therapy. *ACS Nano* **2021**, *15*, doi:10.1021/acsnano.1c00380.

60. Payen, V.L.; Mina, E.; Van Hée, V.F.; Porporato, P.E.; Sonveaux, P. Monocarboxylate transporters in cancer. *Mol. Metab.* 2020, *33*.

61. Yu, S.; Wu, Y.; Li, C.; Qu, Z.; Lou, G.; Guo, X.; Ji, J.; Li, N.; Guo, M.; Zhang, M.; et al. Comprehensive analysis of the SLC16A gene family in pancreatic cancer via integrated bioinformatics. *Sci. Rep.* **2020**, *10*, doi:10.1038/s41598-020-64356-y.

62. Wong, R.S.Y. Apoptosis in cancer: From pathogenesis to treatment. *J. Exp. Clin. Cancer Res.* 2011, *30*.

63. Kumari, R.; Jat, P. Mechanisms of Cellular Senescence: Cell Cycle Arrest and Senescence Associated Secretory Phenotype. *Front. Cell Dev. Biol.* 2021, *9*.

64. Meulmeester, E.; Jochemsen, A. p53: A Guide to Apoptosis. *Curr. Cancer Drug Targets* **2008**, *8*, doi:10.2174/156800908783769337.

65. Rayess, H.; Wang, M.B.; Srivatsan, E.S. Cellular senescence and tumor suppressor gene p16. *Int. J. Cancer* **2012**, *130*, doi:10.1002/ijc.27316.

66. Hashim, N.A.A.; Ab-Rahim, S.; Suddin, L.S.; Saman, M.S.A.; Mazlan, M. Global serum metabolomics profiling of colorectal cancer. *Mol. Clin. Oncol.* 2019, *11*.

67. Vermeulen, K.; Berneman, Z.N.; Van Bockstaele, D.R. Cell cycle and apoptosis. *Cell Prolif.* 2003, *36*.

68. Menendez, D.; Inga, A.; Resnick, M.A. The expanding universe of p53 targets. *Nat. Rev. Cancer* 2009, *9*.

69. Vousden, K.H.; Prives, C. Blinded by the Light: The Growing Complexity of p53. *Cell* 2009, *137*.

70. Haley, V.L.; Barnes, D.J.; Sandovici, I.; Constancia, M.; Graham, C.F.; Pezzella, F.; Bühnemann, C.; Carter, E.J.; Hassan, A.B. Igf2 pathway dependency of the Trp53 developmental and tumour phenotypes. *EMBO Mol. Med.* **2012**, *4*, doi:10.1002/emmm.201101105.

71. Chen, K.L.; Wang, H.L.; Jiang, L.Z.; Qian, Y.; Yang, C.X.; Chang, W.W.; Zhong, J.F.; Xing, G.D. Heat stress induces apoptosis through disruption of dynamic mitochondrial networks in dairy cow mammary epithelial cells. *Vitr. Cell. Dev. Biol. - Anim.* **2020**, *56*, doi:10.1007/s11626-020-00446-5.

72. Khan, A.; Khan, M.Z.; Dou, J.; Umer, S.; Xu, H.; Sammad, A.; Zhu, H. Bin; Wang, Y. RNAi-Mediated Silencing of Catalase Gene Promotes Apoptosis and Impairs Proliferation of Bovine Granulosa Cells under Heat Stress. *Anim. 2020, Vol. 10, Page 1060* **2020**, *10*, 1060, doi:10.3390/ANI10061060.

73. Chen, S.; Zhou, Y.; Chen, Y.; Gu, J. Fastp: An ultra-fast all-in-one FASTQ preprocessor. In Proceedings of the Bioinformatics; 2018; Vol. 34.

74. McCarthy, D.J.; Chen, Y.; Smyth, G.K. Differential expression analysis of multifactor RNA-Seq experiments with respect to biological variation. *Nucleic Acids Res.* **2012**, *40*, doi:10.1093/nar/gks042.

 doi:10.20944/preprints202204.0248.v1

75. Pang, Z.; Chong, J.; Zhou, G.; De Lima Morais, D.A.; Chang, L.; Barrette, M.; Gauthier, C.; Jacques, P.É.; Li, S.; Xia, J. MetaboAnalyst 5.0: Narrowing the gap between raw spectra and functional insights. *Nucleic Acids Res.* **2021**, *49*, doi:10.1093/nar/gkab382.